INVESTIGATING SAND SOURCES AND ORIGINS IN AEOLIS DORSA, MARS, VIA QUANTITATIVE GIS TECHNIQUES. A. S. Boyd[1], D. M. Burr[1], and L. T. Tran[2], [1]Department of Earth and Planetary Sciences, [2]Department of Geography, University of Tennessee, Knoxville, TN. (aboyd21@utk.edu)

Introduction: The widespread distribution of sand on Mars [1-3] prompts the question of its source(s), or regions from which it has been transported, and more fundamentally, its genetic origin(s). At present, sand sources have been resolved in cases where sources lie close to the visible sand deposit [e.g., 4-6], but the sources of many sand deposits on Mars remain unresolved.

This study investigates the potential origins and source regions of sand deposits in the Aeolis Dorsa (AD) region of Mars. AD is located just north of the highland-lowland boundary (HLB)] and includes the twin plateaus Aeolis and Zephyria Plana (Fig. 1a). These plana comprise the westernmost extent of the Medusae Fossae Formation [MFF; e.g., 7, 8], the first of two bedrock units in this study area. The MFF is a layered unit that is hypothesized to be volcaniclastic in origin [e.g., 8, 9]. The second bedrock unit consists of blocky massifs located primarily in the AD southern depression (Fig. 1a). A low-elevation medial basin ('AZP medial basin'; Fig. 1a) separates Aeolis and Zephyria Plana. Both dark and dust-covered sand deposits are found within AD. Transverse dunes, scour marks, and wind streaks co-occur with some of these sand deposits.

The location of AD suggests four potential sources for AD sand: the MFF itself, Elysium Mons to the north, the Cerberus plains to the east, and the highlands to the south. The first three of these source regions would also point to a primary igneous origin for the sand. The goal of this work is to determine whether sand deposits in AD originate from the MFF, and/or are sourced from any surrounding region(s). We are addressing this question via quantitative analysis of sand distribution and inferred wind directions from aeolian features.

Hypotheses: Regional geology supports four working hypotheses for AD sand source(s) (Fig. 1a):

1. Elysium Mons: AD sand could originate as sand-sized volcaniclastic sediments from Elysium Mons or via erosion of effusive Elysium lava flows. Southward transport of these sediments to AD would result in aeolian feature orientations indicative of southward winds, e.g., scour marks on the north sides of obstacles. Sand would likely be concentrated in the north of AD and/or in the AZP medial basin.

2. Cerberus plains lavas: Impact cratering and/or [potentially ongoing; 10] seismic activity in the Cerberus plains (CP) to the east of AD might both produce sand-sized sediment derived from extensive CP lavas [11]. High sand concentrations on the eastern side of Zephyria Planum, co-located with aeolian features indicating westward winds, would support this hypothesis.

3. Southern highlands: Dark sand occurs on the southern highlands south of AD [1, 12]. This sand may be transported northward across the HLB into lower-elevation AD. If AD sand is coming from the southern highlands, a higher concentration of sand should occur in the southern depression, with aeolian features indicating northward transport winds.

4. In situ bedrock weathering: Bedrock weathering occurs in the southern depression and on the two plana. If sand is concentrated on the two plana, and inferred wind directions appear to be locally controlled rather than favoring an external source, then the MFF and/or the blocky massifs may be source(s) of AD sand.

Data and methods: We are mapping sand deposits and associated aeolian features in ArcMap on a 6-m/px-resolution basemap of visible-wavelength images from the Mars Reconnaissance Orbiter Context Camera [CTX; 13]. High-Resolution Imaging Science Experiment [HiRISE; 14] images are used to identify smaller aeolian features. Mars Orbiter Laser Altimeter [MOLA; 15] elevation data are used to constrain potential topographic controls on sand distribution. Sand deposit mapping is being conducted at a scale of ~1:100,000. Sand deposits are recorded as polygons within one of four classifications: dark sand sheets, partially dust-covered sand, dust-covered (bright) sand, and dark sand within bedrock troughs (Fig. 1a). Sand deposits in troughs are mapped separately because their small size makes mapping individual deposits difficult, but their clustering tendency makes mapping groups of such deposits practical. Additional data are recorded in an attribute table in a binary system (Table 1). These data include the presence/absence of dunes, scour marks, wind streaks, and dark bedrock erosion, along with each feature's orientation. Orientations are recorded as any combination of N, S, E, and W, where, e.g., "N" = 315°-045°, "E" = 045°-135°, "S" = 135°-225°, "W" = 225°-315°, "NW" = 225-045°, "NE" = 315-135°, "N 180°" = 270-045°, etc.

We are analyzing the geospatial distribution of sand deposits via two different approaches. In the first approach, we will apply three methods: Average Nearest Neighbor; Ripley's K function; and quadrat overlay on the centroids of sand deposits to analyze their clustering and/or geospatial distribution. With the second approach, we will utilize a moving-window technique to derive various attributes of sand deposits and create multiple raster layers (i.e., lattice

Table 1. Simplified attribute table with information regarding mapped sand deposits. See text for orientation information.

Feature type	Length (m)	Area (m)	Scour marks:	N	E	S	W	NW	NE	N 180°	Tr. dunes:	E-W	N-S	Wind-streaks:	Extending to S	Following troughs	Bedrock erosion
dark sand in trough	6.97E+03	2.49E+06									1						
dark sand	2.98E+04	1.20E+07	1	1						1				1	1		1
dark sand	1.40E+04	9.29E+06									1		1	1	1		1
dark sand	4.99E+04	5.18E+07	1				1	1		1				1	1		

data) for these attributes. We will apply several spatial statistical tools suitable to lattice data (e.g., global and local Moran's I, Getis-Ord's G statistic) on those raster layers to explore spatial pattern and/or distribution of sand deposits and their attributes (e.g., size, shape, orientation). Finally, we will compare the results from the approaches on their usefulness in exploring sand deposits and similar features on Mars.

Preliminary results: Preliminary mapping has been completed over ~70% of AD. Most sand appears to be located upon, or at the edges of, Aeolis and Zephyria Plana. The AZP medial basin is largely devoid of sand. The confinement of sand largely to Aeolis and Zephyria Plana may be due to (1) sand being sourced dominantly from the MFF, or (2) that the two plana acting as effective sand traps.

Most scour marks wrap around the northerly sides of obstacles (Fig. 1b). Wind streaks occur primarily in bedrock troughs, extending southward (Fig. 1c). These features indicate locally variable winds, but regional dominance of southward-directed winds. The regional southward trend may be due to (1) dominant winds coming from the north, or (2) winds controlled by local N-S trending topography.

In the southern depression, some sand is eroding in situ from dark layers in the massifs. Although the southern depression shows substantial bedrock erosion, it is ~500 m lower than elsewhere in AD, and sand sourced from the massifs is unlikely to travel out of the southern depression. Thus, although massifs are sourcing sand within the southern depression, source(s) of sand elsewhere in AD remain unresolved. We will complete mapping and data analyses, and subsequently evaluate the relative likelihood of sand sources based on our analyses and observations. The results of this study will be used in conjunction with spectral analyses and climate models to further constrain the likely contributions of various potential AD sand sources and origins.

References: [1] Hayward R. K. et al. (2007) *JGR*, *112*, E11007. [2] Hayward R. K. et al. (2009) *JGR*, *114*, E11012. [3] Hayward R. K. et al. (2014) *Icarus*, *230*, 38-46. [4] Langevin Y. et al. (2005) *Sci*, *307*, 1584-6. [5] Mangold N. et al. (2007) *JGR*, *112*, E08S04. [6] Chojnacki M. et al. (2014) *Icarus*, *232*, 187-219. [7] Sakimoto S. E. H. et al. (1999) *JGR*, *104*, E10. [8] Bradley B. A. et al. (2002) *JGR*, *107*, E8. [9] Mandt K. E. et al. (2008) *JGR*, *113*, E12011. [10] Roberts G. P. et al. (2012) *JGR*, *117*, E02009. [11] Keszthelyi L. et al. (2004) *G3*, *5*. [12] Tirsch D. et al. (2011) *JGR*, *116*, E03002. [13] Malin M. C. and Edgett K. S. (2001) *JGR*, *106*, 23429-570. [14] McEwen A. S. et al. (2007) *JGR*, *112*, E05S02. [15] Smith D. E. et al. (2001) *JGR*, *106*, 23689-23722.

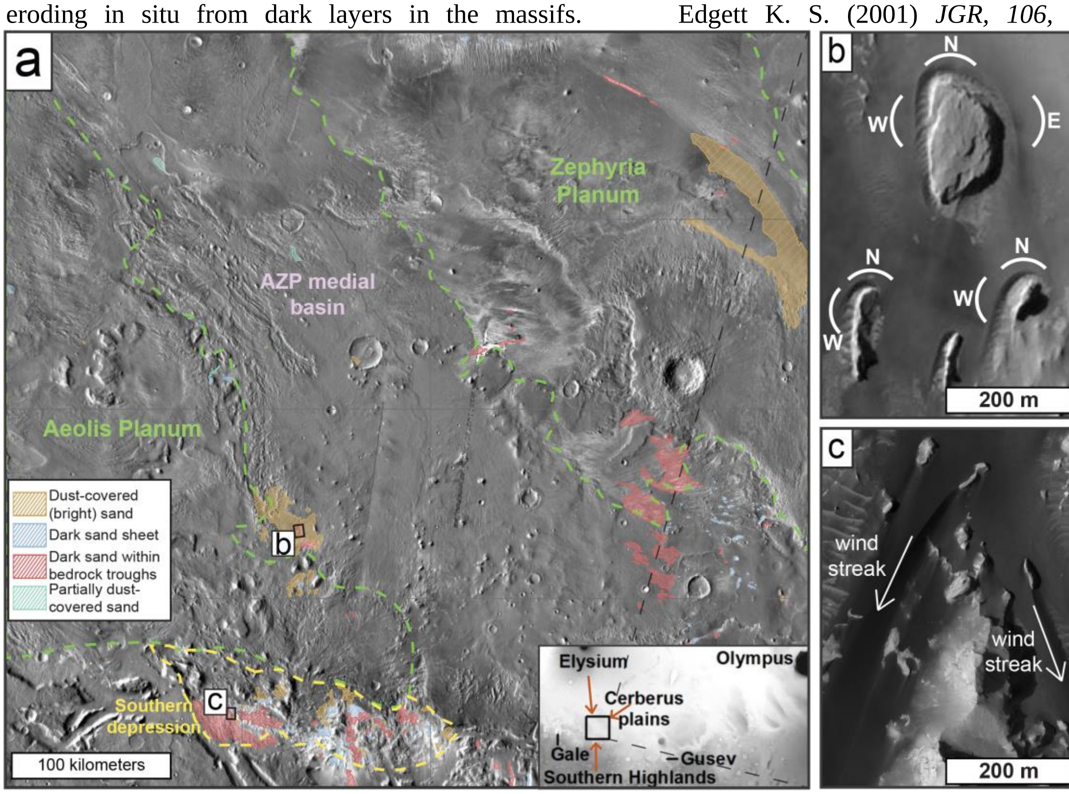

Figure 1. a) CTX basemap of AD showing initial sand mapping and notable landforms. Inset shows regional context and external potential sand sources. b) Scour marks with denoted orientations. Arced lines represent extent of lettered compass direction. c) Wind streaks (white arrows denote orientation). (Credit, b & c: NASA/JPL/Univ. of AZ)